Supplement of Atmos. Chem. Phys., 24, 8507–8518, 2024
https://doi.org/10.5194/acp-24-8507-2024-supplement

Atmospheric Chemistry and Physics
Open Access

Supplement of

Characterizing water solubility of fresh and aged secondary organic aerosol in $PM_{2.5}$ with the stable carbon isotope technique

Fenghua Wei et al.

Correspondence to: Xing Peng (pengxing@pku.edu.cn)

Contents of this file

S1: PMF model and results

In this study, the PMF model (EPA PMF v5.0) was employed to identify the sources of TC and WSOM. The detailed fundamental principle of this model can be found in Paatero and Tapper. (1994). The mass concentration and uncertainty matrixes of seventeen indicative chemical components (OM, EC, NH_4^+, Cl^-, NO_3^-, SO_4^{2-}, Na, Mg, Al, K, Ca, V, Ni, Cd, Fe, Zn, and Pb) were put into this model to identify the $PM_{2.5}$ sources. The measuring methods for each component are described in the main text, and the measurement processes were subjected to strict quality control as follows, which are also available in our previous studies (Huang et al., 2019; Yan et al., 2022). The OC/EC analyzer was calibrated using eight standard concentration gradients of sucrose solution prior to each sample analysis of the carbonaceous fractions, with all standard curves achieving an R^2 value exceeding 0.999. The charge concentration balance of water-soluble ions (R^2 = 0.98, slope = 0.87) confirmed the validity of the measurement results for water-soluble ions. The spiked recoveries for all metal elements ranged between 80 % and 120 % in this study. Furthermore, the background concentration of blank samples and the reproducibility of the measurement results were evaluated during the determination of each component, and all the results met the experimental requirements.

To find out the optimal solution, factor numbers ranging from 5 to 11 were evaluated using the PMF model. Among them, the nine-factor solution exhibited a notable covariance between vehicle emissions and biomass burning sources, while the eleven-factor solution displayed a dispersed distribution of Pb, Fe and Cd. Subsequently, the ten-factor solution was identified as optimal due to its highly interpretable factor profiles (Fig. S2), with scaled residuals demonstrating a generally symmetrically distribution between −3 and +3. There was a strong correlation between the total mass of the input species and the

total mass of all the model-reconstructed factors (R^2 = 0.99, slope = 1.04) (Fig. S3), and favorable correlations were also observed between the source contributions and their corresponding source markers (R^2 = 0.83 ~ 0.96), suggesting robust performance of PMF model. According to Fig. S2, factor 1 exhibited high percentage explained variation (EV) values for SO_4^{2-} (66 %) and NH_4^+ (59 %. In factor 2, not only OM and EC displayed substantial EV values (49 % and 62 %), Zn and Fe also contribute notably. Factor 3 demonstrated the highest EV values for the elements Na and Mg. Cl^- in factor 4 had an EV value of up to 82 %. NO_3^- (67 %) and NH_4^+ (25 %) exhibited the highest EV values in factor 5. Factor 6 showed the highest EV values for Pb, Cd and Zn, while factor 7 demonstrated the highest EV values for V and Ni. Factors 8 ~ 10 exhibited the highest EV values for Ca (73 %), K (72 %) and Al (76 %), respectively. Consequently, the ten factors were identified as secondary sulfate, vehicle emissions, aged sea salt, coal combustion, secondary nitrate, industrial emissions, ship emissions, construction dust, biomass burning, and fugitive dust, respectively. SOA was then estimated from the OM fraction in both secondary sulfate and secondary nitrate factors. To compare with BSIM results, the source apportionment of TC was merged into three sources, including SOA, traffic emission, and biomass burning (Fig. S4) (Zong et al., 2018). The industrial emission source and coal combustion source were not included because of their little contribution to carbonaceous fraction. The remaining eight sources were then reapportioned and then combined according to the contribution to OC and EC. Specifically, the contributions of vehicle and ship emissions to EC and OC were attributed to the traffic source. The contributions of secondary sulfate, secondary nitrate, and aged sea salt sources to OC were all attributed to the SOA. The contributions of biomass burning source to OC were attributed to the BB (biomass burning) source.

In the source apportionment of WSOC, the mass concentration and uncertainty matrixes of five species (CO_2^+, $C_4H_9^+$, $C_2H_4O_2^+$, WSOC, and WSOO) were put into the PMF model to identify and

calculate source contributions to WSOC. Following examination of a range of 2 to 4 factor numbers, a three-factor solution output by the PMF model was determined to be optimal. The scaled residuals exhibited a generally symmetrical distribution between -3 and +3 as well. Moreover, there was also a strong overall correlation between the total factor concentrations reconstructed by the PMF model and the total mass concentrations of the measured species (R^2 = 0.99, slope = 0.97) (Fig. S3). According to Fig. S5, factor 1 displayed the highest percentage of EV values for *m/z 44* (CO_2^+) and WSOO (73 % and 63 %, respectively), with an oxygen-carbon ratio (O/C) of 1.01, which is highly oxidized and identified as aged SOC source. Factor 2 exhibited EV values of 64% for *m/z 57* ($C_4H_9^+$), 29% for WSOC, 27% for *m/z 44*, and 23% for WSOO. In addition, factor 2 had a lower level of oxidation with an O/C ratio of 0.43, and was therefore identified as fresh SOC source. Factor 3 demonstrated a 100 % EV value for *m/z 60* ($C_2H_4O_2^+$) and a low O/C ratio of 0.36, indicating that factor 3 represented the biomass burning source (BB).

S2: Sampling of potential emission sources of carbonaceous aerosol

$PM_{2.5}$ samples of four sources were collected from ambient air and simulation experiments to measure the $\delta^{13}C$ values of TC and WSOC in this study. We collected $PM_{2.5}$ samples from two tunnel sites (Mount Tanglang tunnel and Jiuweiling tunnel), which can comprehensively reflect the vehicle emissions level to ambient air in Shenzhen because of its specificity of the environment. Two medium-flow samplers (KC-120H model, Qingdao Laoshan, 100 L/min) were used in this sampling process. The lengths of those two tunnels were 1711 m and 1447 m, representing the emission characteristics of diesel and petrol vehicles in Shenzhen respectively. Specifically, six samples were obtained from 23:00 to 02:10 and 02:30 to 05:30 on 13-18 October 2014 at the Mount Tanglang tunnel site. Additional eight samples were subsequently collected at different periods (peak and off-peak traffic periods in both daytime and night)

on 20-22 January 2015 at the junction of one side of Mount Tanglang tunnel, and the sampling durations ranged from 2.5 to 11.5 hours. A total of 11 samples were obtained at the Jiuweiling tunnel site. The peak and off-peak traffic periods in both daytime and night were also included in this sampling period, and the sampling durations ranged from 2 to 6 hours. Fore fresh SOA, five $PM_{2.5}$ samples from petrol vehicle bench tests conducted under different fuel types and operating conditions were collected. Detailed information about this test system was displayed in Zheng et al. (2017) (Zheng 2017). Two parallel samples were collected and measured under each operating condition to ensure the reliability of the measured data. Two aged SOA samples were collected at the national ambient air background monitoring station in Mount Wuzhi, Hainan Province, from 13-15 April 2015. A complete secondary transport process was captured during this sampling period, and each sampling duration was 23.5 hours. Lastly, We collected three $PM_{2.5}$ samples representing the biomass combustion source through biomass combustion simulation experiment (He et al., 2010), of which were conducted in the combustion simulation laboratory at Peking University Shenzhen Graduate School on 24-28 May 2017. Pine branches, as a major source of biomass burning in south China (Chen et al., 2017) were selected as the representative plant for the combustion simulation experiment in this study. The pine branches were divided into three weight groups (low (3 kg), medium (6 kg) and high (8 kg)). Samples at three different combustion stages (ignition, flame combustion, and complete combustion) were collected, and the sampling time at each stage was 49, 75, and 90 minutes, respectively. Each sampling and analysis process was repeated three times to ensure reliability.

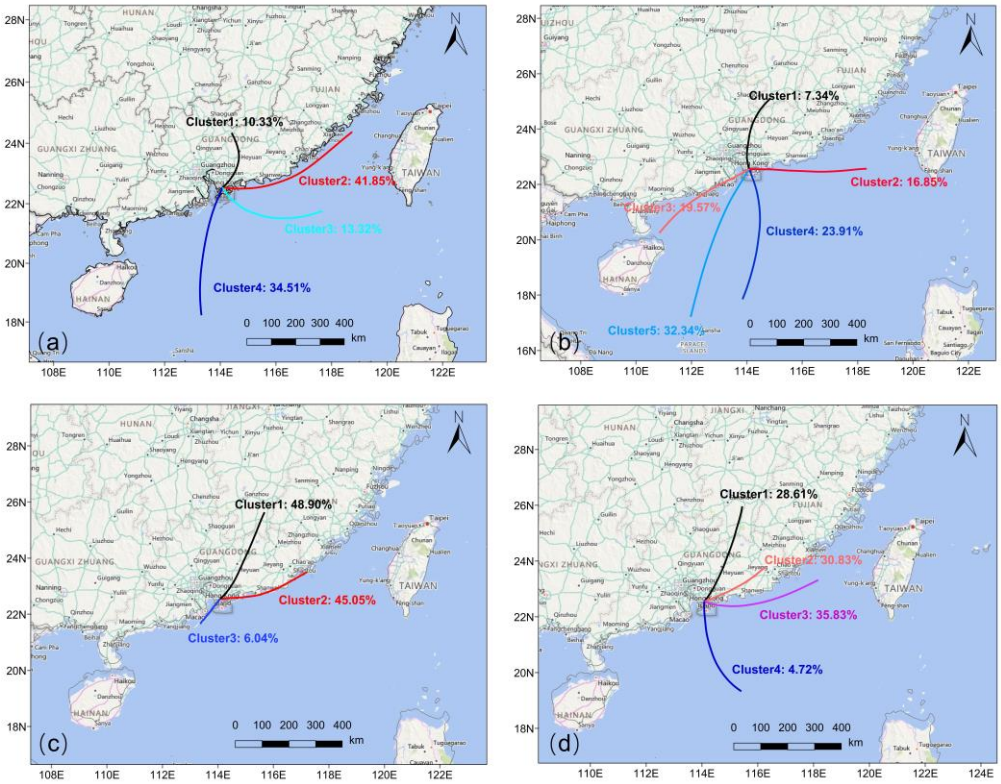

102

103 **Figure S1.** Seasonal backward trajectory of air masses in Shenzhen, 2019. (a) spring (b) summer (c) fall

104 (d) winter. Map image: © Microsoft by MeteoInfoMap.

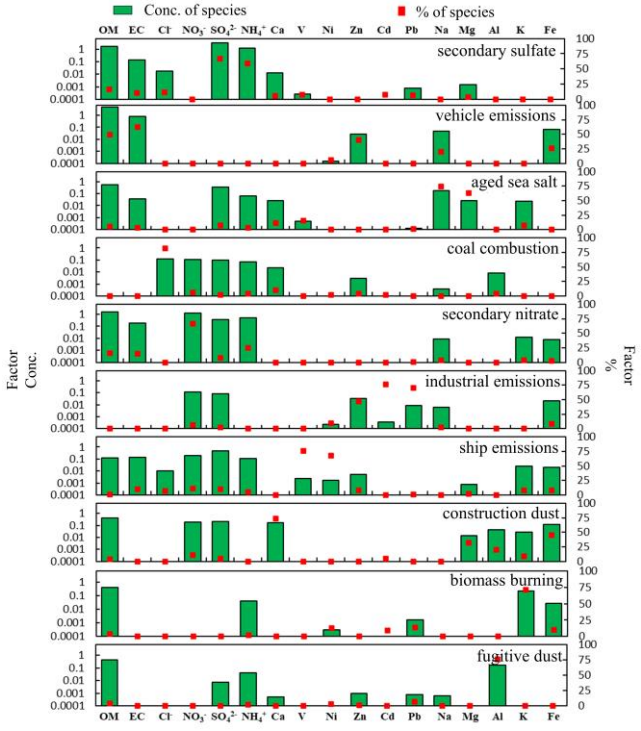

105

106 **Figure S2.** The source profiles resolved by PMF for $PM_{2.5}$.

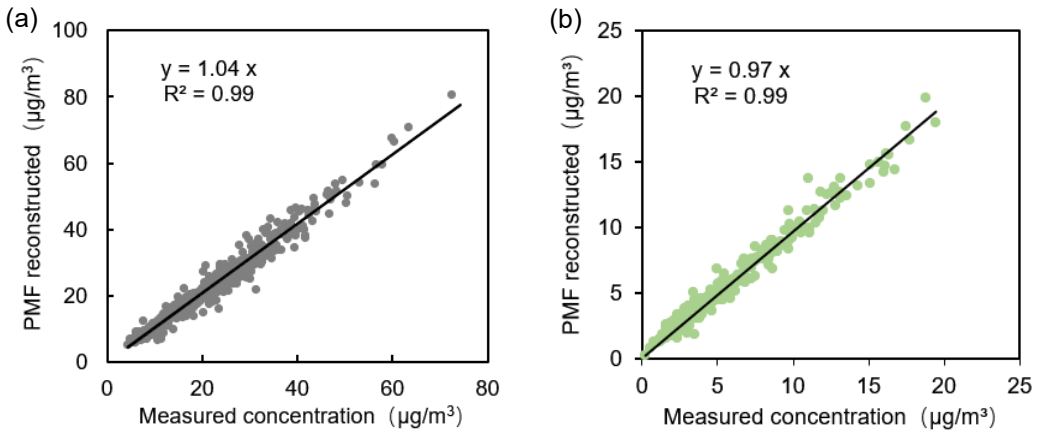

107

108 **Figure S3.** Comparison between the measured total mass of species and the PMF reconstructed total

109 mass of sources of (a) $PM_{2.5}$, (b) WSOC.

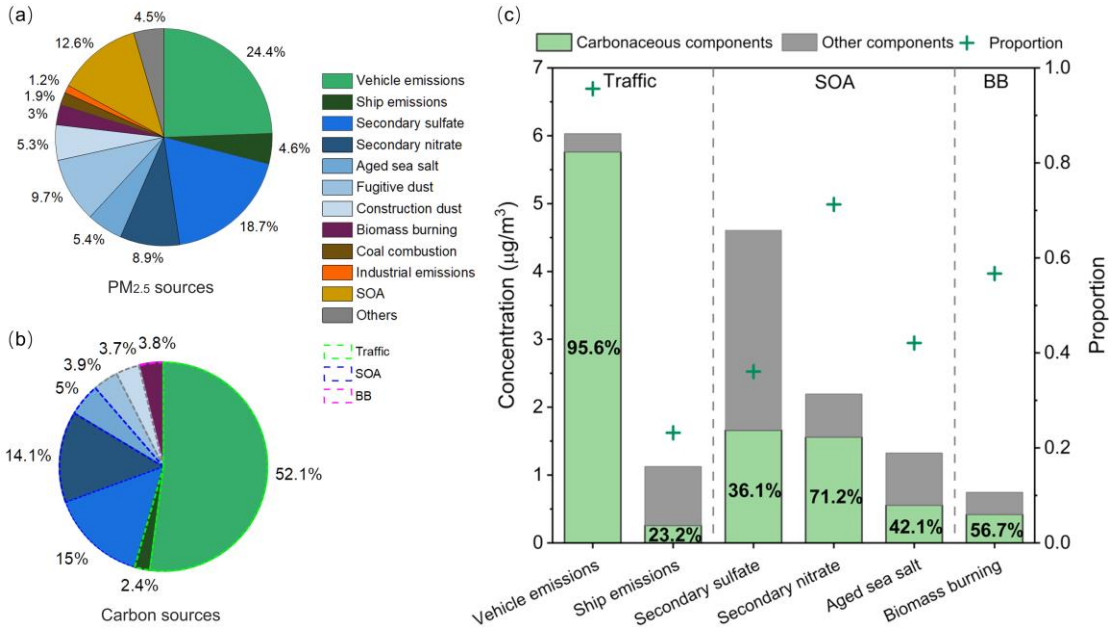

110

111 **Figure S4.** The relative contribution of different sources to $PM_{2.5}$ (a) and carbonaceous aerosol (b) based

112 on the PMF model. (c) The contribution of different sources to $PM_{2.5}$ and carbonaceous aerosol.

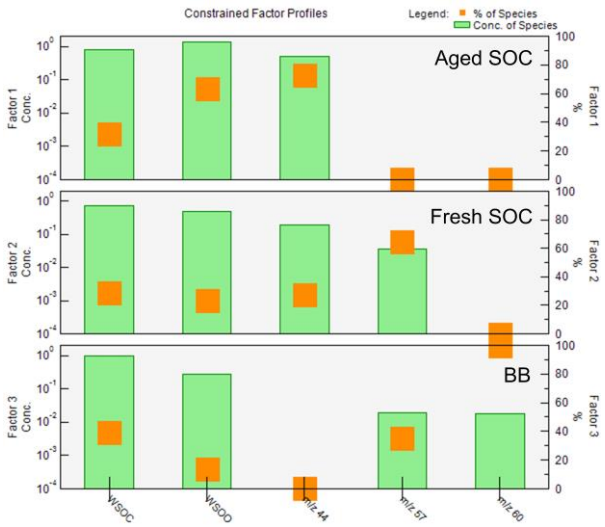

Figure S5. The source profiles resolved by PMF for WSOC.

Table S1. Description of the sampling sites in Shenzhen.

Site	Site Code	Coordinates	Site description	
University town	UT	Lat: 22.59°N Long: 113.97°E	Urban	This site reflects the pollution characteristics of typical urban areas and regional transport
Longhua	LH	Lat: 22.68°N Long: 114.01°E	Urban	This site generally reflects the pollution characteristics of urban local emissions
Honghu	HH	Lat: 22.57°N Long: 114.14°E	Urban	This site reflects the pollution characteristics of the general urban areas
Xixiang	XX	Lat: 22.58°N Long: 113.90°E	Urban	This site reflects the pollution characteristics of western industrial urban areas in Shenzhen
Dapeng	DP	Lat: 22.64°N Long: 114.42°E	Background	This site reflects the pollution characteristics of the eastern coastal tourist areas

Table S2. General meteorological conditions during the sampling period in 2019.

	Mean temp. (℃)	Rainfall (mm)	Mean RH (%)	Mean wind speed (m s-1)	Predominant wind direction
Spring (1 Mar-8 Apr)	21.3	151.8	83.0	1.7	ESE
Summer (1 Jun-3 Jul)	28.5	275.8	85.0	2.2	SW
Autumn (1 Sept-11 Oct)	27.6	175.0	74.0	1.6	ESE
Winter (22 Nov-30 Dec)	19.5	3.2	62.0	2.0	NNE

Table S3. Comparison of $\delta^{13}C_{TC}$ source signatures in this study with global datasets.

Emission sources	Continent	Location	Sample types	$\delta^{13}C$(‰)	SD	Ref.
	Asia(This study)	**China, Shenzhen**	**Traffic**	**-26.26**	**0.50**	**-**
	Asia	China	Wucun Tunnel, Entrance	-25.84	0.23	(Yao et al., 2022)
	Asia	China	Wucun Tunnel, Exit	-25.88	0.24	
	Asia	China	Xianyueshan Tunnel, Entrance	-25.88	0.26	
	Asia	China	Xianyueshan Tunnel, Exit	-25.79	0.23	
	Asia	China, Guangzhou	Traffic	-24.6 to -25.5		(Dai et al., 2015)
	Asia	India	Traffic	-25.3	0.3	(Agnihotri et al., 2011)
	Asia	Nepal	Traffic	-26.5 to -26.1		(Shakya;Ziemba and Griffin 2010)
	Asia	China	Traffic	-25.85	0.22	(Yao et al., 2022)
	Asia	China	Traffic	-25.27	0.32	(Chen et al., 2012)
Traffic	Asia	Pearl River Delta	Gasoline exhaust	-28.6	0.6	
	Asia	Pearl River Delta	Diesel exhaust	-27.8	0.2	
	Asia	China	Zhujiang Tunnel, Vehicle emissions	-25	0.3	(Dai et al.,2013)
	Asia	India	Diesel exhaust	-26.3	0.2	
	Asia	India	Bio-diesel exhaust	-26.5	0.1	(Singh et al., 2018)
	Asia	India	Petrol(Gasoline) exhaust	-26.1	0.01	
	North America	Mexico	Tunnel; Diesel vehicle emissions	-24.6	0.3	(López-Veneroni 2009)
	North America	Mexico	Tunnel; Gasoline vehicle emissions	-25.5	0.1	
	Oceania	New Zealand	Mount Victoria Tunnel	-25.9	0.8	(Ancelet et al., 2011)
	Europe	Germany	Gasoline exhaust	–26.2	0.2	(Fisseha et al., 2009)
	Europe	Paris	Diesel exhaust	–26.5	0.5	(Widory et al., 2004)
	Europe	Germany	Diesel exhaust	–27.6	0.01	(Fisseha et al., 2009)
	Europe	Paris	Complete combustion of diesel	-29		(Widory 2006)

	Europe	Paris	Complete combustion of gasoline	-27		(Widory 2006)
	Europe	Paris	Fuel oil exhaust	–26.5	0.5	(Widory et al., 2004)
	Europe	Krakow, Poland	Traffic	-30	1	(Zimnoch et al., 2020)
	worldwide	worldwide	Traffic group1	-26.8	1.1	
	worldwide	worldwide	Traffic group2	-28.9	1.7	(Yao et al., 2022)
	worldwide	worldwide	Traffic group3	30.2	0.9	
SOA	**Asia(Our study)**	**China, Hainan**	**Aged SOC , ambient samples of the Mount Wuzhi**	**-25.54**	**0.28**	**-**
	Asia(Our study)	**China, Shenzhen**	**Fresh SOC , petrol vehicle bench tests**	**-27.31**	**0.73**	
	Europe	Germany	Compounds in SOA: aerosol-phase nopinone	-27.6 to -24.8		
	Europe	Germany	Compounds in SOA: acetone	-35.1 to -38.6		
	Europe	Germany	Compounds in SOA: gas-phase nopinone	-28.8		(Fisseha et al., 2009)
	Europe	Germany	Precursor of SOA: initial β-pinene injected	-30.1		
	Europe	Germany	Precursors of SOA	-29.6	0.2	
	North America	Canada	Secondary particulate organic matter			(Irei et al., 2011)
	North America	Canada,	Secondary particulate organic matter	-32.2 to -32.9		(Irei et al., 2006)
BB	**Asia(Our study)**	**China, Shenzhen**	**Burning experiment results of pine branches**	**-27.58**	**0.24**	**-**
	worldwide	worldwide	C3 plant	-27.2	1.6	
	Asia	China	C3 plant	-27.89	0.26	(Yao et al., 2022)
	Asia	China	Seven C3 plants	-27.12		
	Asia	China	Biomass burning (Seven C3 plants)	-26.99	1.11	
	America	Texas	C3 plant	-27	6	(Boutton 1991)
	Europe	Krakow, Poland	Biomass burning(C3 plants)	-26	2	(Zimnoch et al., 2020)
	Asia	China	C4 smoldering	-14.25		
	Asia	China	C4 flaming	-18.42		
	Asia	China	C4 plant (corn stalk)	-12		(Yao et al., 2022)
	Asia	China	Biomass burning (corn stalk)	-13.09		
	worldwide	worldwide	C4 plant	-13.2	1.1	
	America	Texas	C4 plant	-13	4	(Boutton 1991)

References

Agnihotri, R., Mandal, T. K., Karapurkar, S. G., Naja, M., Gadi, R., Ahammmed, Y. N., Kumar, A., Saud, T. and Saxena, M.: Stable carbon and nitrogen isotopic composition of bulk aerosols over India and northern Indian Ocean, Atmos. Environ., 45, 2828-2835, 2011.

Ancelet, T., Davy, P. K., Trompetter, W. J., Markwitz, A. and Weatherburn, D. C.: Carbonaceous aerosols in an urban tunnel, Atmos. Environ., 45, 4463-4469, 2011.

Boutton, T. W.: 11-Stable carbon isotope ratios of natural materials: II, atmospheric, terrestrial, marine, and freshwater environments, Carbon Isotope Techniques., 274, 1991.

Chen, Y., Wenger, J. C., Yang, F. M., Cao, J. J., Huang, R. J., Shi, G. M., Zhang, S. M., Tian, M. and Wang, H. B.: Source characterization of urban particles from meat smoking activities in Chongqing, China using single particle aerosol mass spectrometry, Environ. Pollut., 228, 92-101, 2017.

Chen, Y. J., Cai, W. W., Huang, G. P., Li, J. and Zhang, G.: Stable carbon isotope of black carbon from typical emission sources in China, Environ. Sci., 33, 673-678, 2012.

Dai, S., Bi, X., Chan, L. Y., He, J., Wang, B., Wang, X., Peng, P., Sheng, G. and Fu, J.: Chemical and stable carbon isotopic composition of $PM_{2.5}$ from on-road vehicle emissions in the PRD region and implications for vehicle emission control policy, Atmos. Chem. Phys., 15, 3097-3108, 2015.

Fisseha, R., Spahn, H., Wegener, R., Hohaus, T., Brasse, G., Wissel, H., Tillmann, R., Wahner, A., Koppmann, R. and Kiendler-Scharr, A.: Stable carbon isotope composition of secondary organic aerosol from β-pinene oxidation, J. Geophys. Res. Atmos., 114, D02304, https://doi.org/10.1029/2008JD011326, 2009.

He, L. Y., Lin, Y., Huang, X. F., Guo, S., Xue, L., Su, Q., Hu, M., Luan, S. J. and Zhang, Y. H.: Characterization of high-resolution aerosol mass spectra of primary organic aerosol emissions from Chinese cooking and biomass burning, Atmos. Chem. Phys., 10, 11535-11543, 2010.

Huang, X. F., Zou, B. B., He, L. Y., Hu, M. and Prevot, A. S. H.: Exploration of $PM_{2.5}$ sources on the regional scale in the Pearl River Delta based on ME-2 modeling, Atmos. Chem. Phys., 18 (16), 11563-11580, 2018.

Irei, S., Huang, L., Collin, F., Zhang, W., Hastie, D. and Rudolph, J.: Flow reactor studies of the stable carbon isotope composition of secondary particulate organic matter generated by OH-radical-induced reactions of toluene, Atmos. Environ., 40, 5858-5867, 2006.

Irei, S., Rudolph, J., Huang, L., Auld, J. and Hastie, D.: Stable carbon isotope ratio of secondary particulate organic matter formed by photooxidation of toluene in indoor smog chamber, Atmos. Environ., 45, 856-862, 2011.

López-Veneroni, D.: The stable carbon isotope composition of $PM_{2.5}$ and PM_{10} in Mexico City Metropolitan Area air, Atmos. Environ., 43, 4491-4502, 2009.

Paatero, P. and Tapper, U.: Positive matrix factorization: a nonnegative factor model with optimal utilization of error estimates of data values, Environmetrics., 5, 111-126, 1994.

Shakya, K. M., Ziemba, L. D. and Griffin, R. J.: Characteristics and sources of carbonaceous, ionic, and isotopic species of wintertime atmospheric aerosols in Kathmandu valley, Nepal, Aerosol Air Qual Res., 10, 219-U13, 2010.

Singh, G. K., Rajput, P., Paul, D. and Gupt, T.: Wintertime study on bulk composition and stable carbon isotope analysis of ambient aerosols from North India, J. Aerosol Sci., 126, 231-241, 2018.

Widory, D. Combustibles, fuels and their combustion products: A view through carbon isotopes, Combust. Theory Model., 10, 831-841, 2006.

Widory, D., Roy, S., Le Moullec, Y., Goupil, G., Cocherie, A. and Guerrot, C.: The origin of atmospheric particles in Paris: a view through carbon and lead isotopes, Atmos. Environ., 38, 953-961, 2004.

Yan, R. H., Peng, X., Lin, W., He, L. Y., Wei, F. H., Tang, M. X. and Huang, X. F.: Trends and Challenges regarding the source-specific health risk of $PM_{2.5}$-bound metals in a Chinese megacity from 2014 to 2020, Environ. Sci. Technol., 56 (11), 6996-7005, 2022.

Yao, P., Huang, R. J., Ni, H. Y., Kairys, N., Yang, L., Meijer, H. A. J. and Dusek, U.: ^{13}C signatures of aerosol organic and elemental carbon from major combustion sources in China compared to worldwide estimates, Sci. Total Environ., 810, 151284, https://doi.org/10.1016/j.scitotenv.2021.151284, 2022.

Zheng, J.: Source apportionment of organic aerosols and contribution of secondary formation from vehicle emissions, Peking university, 2017.

Zimnoch, M., Samek, L., Furman, L., Styszko, K., Skiba, A., Gorczyca, Z., Galkowski, M., Rozanski, K. and Konduracka, E.: Application of natural carbon isotopes for emission source apportionment of carbonaceous particulate matter in urban atmosphere: a case study from Krakow, southern Poland, Sustainability-Basel., 12, 5777, https://doi.org/10.3390/su12145777, 2020.

Zong, Z., Tan, Y., Wang, X., Tian, C., Fang, Y., Chen, Y., Fang, Y., Han, G., Li, J. and Zhang, G.:

Assessment and quantification of NO_x sources at a regional background site in North China: Comparative results from a Bayesian isotopic mixing model and a positive matrix factorization model, Environ. Pollut., 242, 1379-1386, 2018.